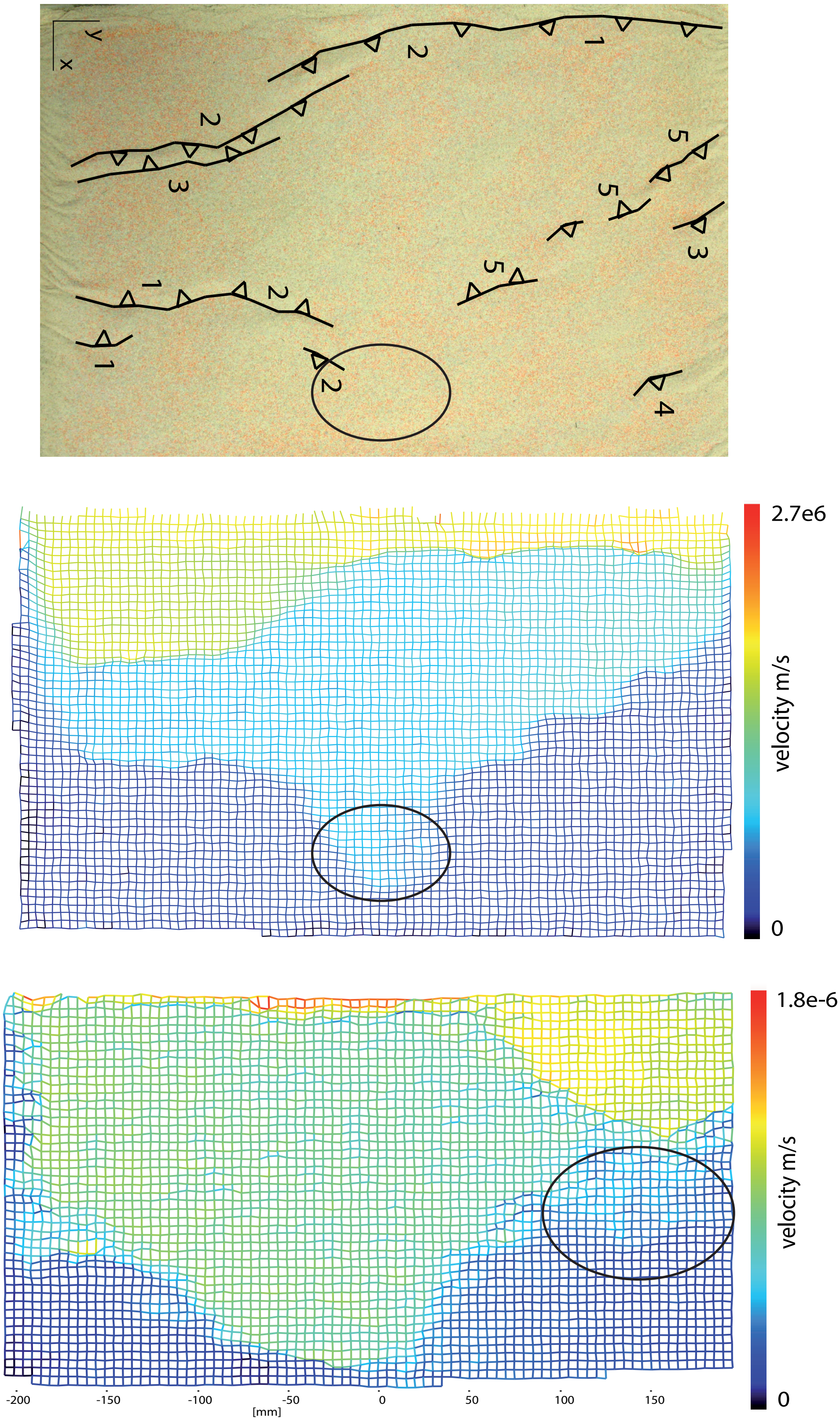

Fig. 8.1a (top), b (center), 8.2 (bottom): a) The experimental surface in top view shows the finite strain pattern after 27.7% of bulk shortening with thrusts numbered in order of appearance. Convergence was in x-direction (from top to bottom). The finite dimensions are 28 cm (x) and 42 cm (y); b) The incremental velocity field of the final stage of Exp. 4 (cf. Chapter 7). The colour contrasts are velocity contrasts, which have sharp boundaries (marked in Fig. 8.1b) and outline the structures where strain localizes (thrusts in Fig. 8.1a, marked). Velocity contrasts indicate the positions of structures before they have actually formed; (cf. Fig. 8.1a); Fig. 8.2: The incremental velocity field of the final stage of Exp. 6 (cf. Chapter 7). Velocity contrasts have diffuse boundaries (marked) unlike Fig. 8.1b. Due to the lack of sharp contacts, the position of future structures cannot be made out beforehand.

8. Additional analogue data

Extensive data sets result from the PIV monitoring of the physical simulations. In the following I point out some interesting data that could be subjects for future studies, as they deal with 1) the variation of deformation modes in time and space (e.g., strain hardening and strain weakening), 2) the aspects of uncertainty due to incomplete data resolution, e.g., for velocity fields, and 3) the interaction and variation of strain accumulation along structures within profiles orogen-normal and orogen-parallel over time.

1) Figure 8.1a shows the real experimental surface, Figure 8.1b the corresponding incremental velocity field of the final stage after 27.7% of bulk shortening (Exp. 4, cf. Chapter 7). Colour contrasts mark locations of velocity changes, where faults localize (i.e., thrusts with oblique components in step-over zones). These velocity contrasts are sharp in Figure 8.1b, and rather diffuse (marked) in the incremental velocity field of Exp. 6 in Figure 8.2 (cf. Chapter 7). Due to this diffuseness the exact position of faults could not be located from the velocity contrasts in the incremental velocity field.

Another obvious feature is the missing coincidence of velocity contrast or gradient development with the actual formation of structures that are visible at the real surface. Instead some time elapse between a diffuse velocity contrast (marked in Fig. 8.1b) and the actual strain localization (marked in Fig. 8.1a) can be noticed. This may be interpreted in terms of initial strain hardening (diffuse strain accumulation) and subsequent strain weakening (localized deformation). A future study should involve an analysis of the time elapsing between stages of different deformation modes.

2) Without proper spatial resolution of the velocity data, velocity contrasts and therefore the structures cannot be precisely located. This problem is also depicted in Figures 8.3 and 8.4 showing that a given dataset can be variously interpreted when the spatial coverage between the data is incomplete. A similar problem can arise for GPS data: without the appropriate GPS station coverage, the data cannot be used for the prediction of deformation events or future structures. However, we have to bear in mind that GPS data also include the elastic component of deformation and record velocity fields for much shorter time spans that are not sampled by the analogue incremental velocity data. Also, lithospheric deformation in nature is certainly more complex than the strain accumulation in the models.

3) Strain data were extracted along profile 1300 (cf. Fig. 8.5 for location) for all 180 time increments equalling 40 Ma in nature, and compiled into a time series of strain profiles (Fig. 8.6). Time increases from top to bottom, and the piston advances from left to right. This motion over time causes all structures to appear obliquely. Strain accumulation is high for dark colours, and low for light grey colours. Thus, the presence of light colours horizontal within dark structures (“zebra pattern”) shows that strain accumulation is not continuous over time, but that there are phases when no or only little strain is accumulated. We can study this variation over time and how the active structures correlate when plotting the incremental vector displacement for some points along the profile (1300) and other profiles (1240, 1270, 1330, 1360, 1390) in a different plot (Fig. 8.7). Figure 8.8 gives an idea how strain accumulation varies along-strike of the orogen within a given structure.

Such temporal patterns might show scale-dependent stages of deformation, each possibly following a particular deformation mode which could also give more information on the underlying deformation framework. In that respect, strain weakening effects are characteristic for the “continuum-Euclidean” framework, strain hardening effects for the block model, and both effects in balance for the fractal complexity (e.g., Ben-Zion and Sammis, 2003).

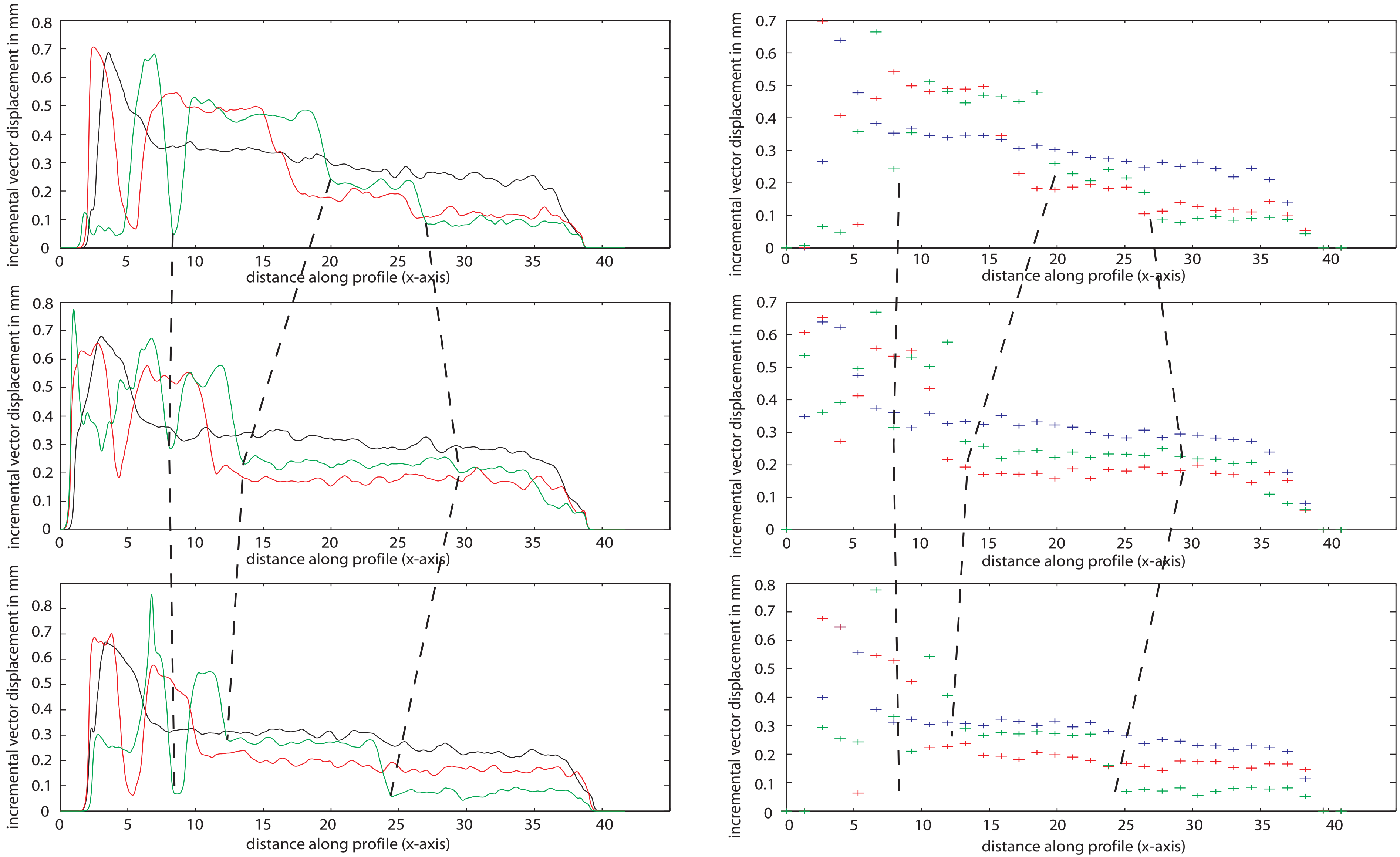

Fig. 8.3: This figure aims to show the difficulties in using velocity gradients to locate active structures in the upper crust and follow them along-strike of the deformation system (black dashed lines), when the data resolution is not good (right: velocity data present for every fifth time increment), compared to the complete coverage (left: velocity data are present for every time increment). Each of the plots gives the information for one profile along-strike of the orogen (Exp. 4, cf. Fig. 7.9a for location of profiles). The colour code for the profiles within one plot indicates the time step (blue: 60, red: 120, green: 180). The x-axis indicates the position of the velocity displacement in the direction of convergence.

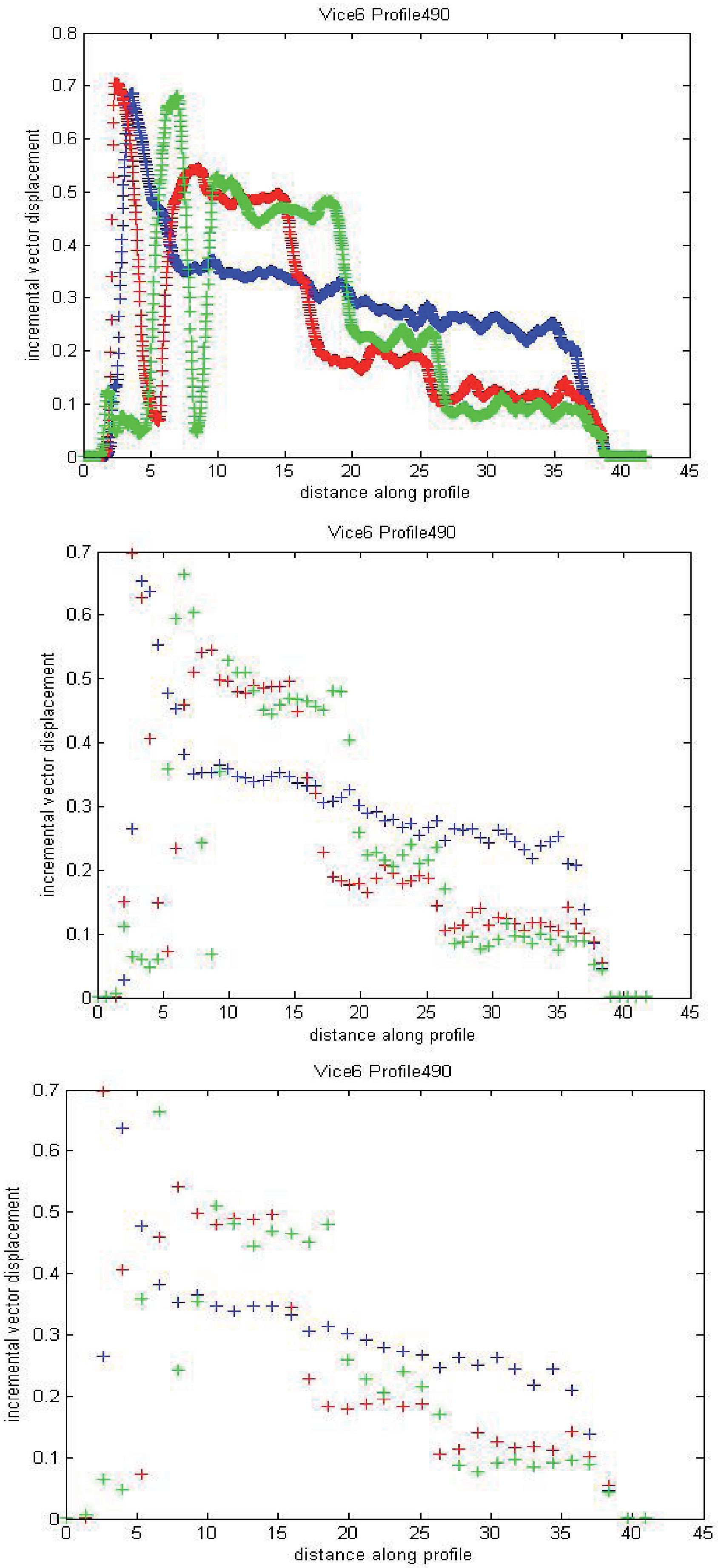

Fig 8.4: These figures again show that extrapolation from few velocity data points (e.g., data from GPS stations) to get a continuous data set is not straightforward and gives more than one option to construct the "real" continuous displacement field. The colour code for the profiles within one plot indicates the time step (blue: 60, red: 120, green: 180). The profile number is given in each plot.

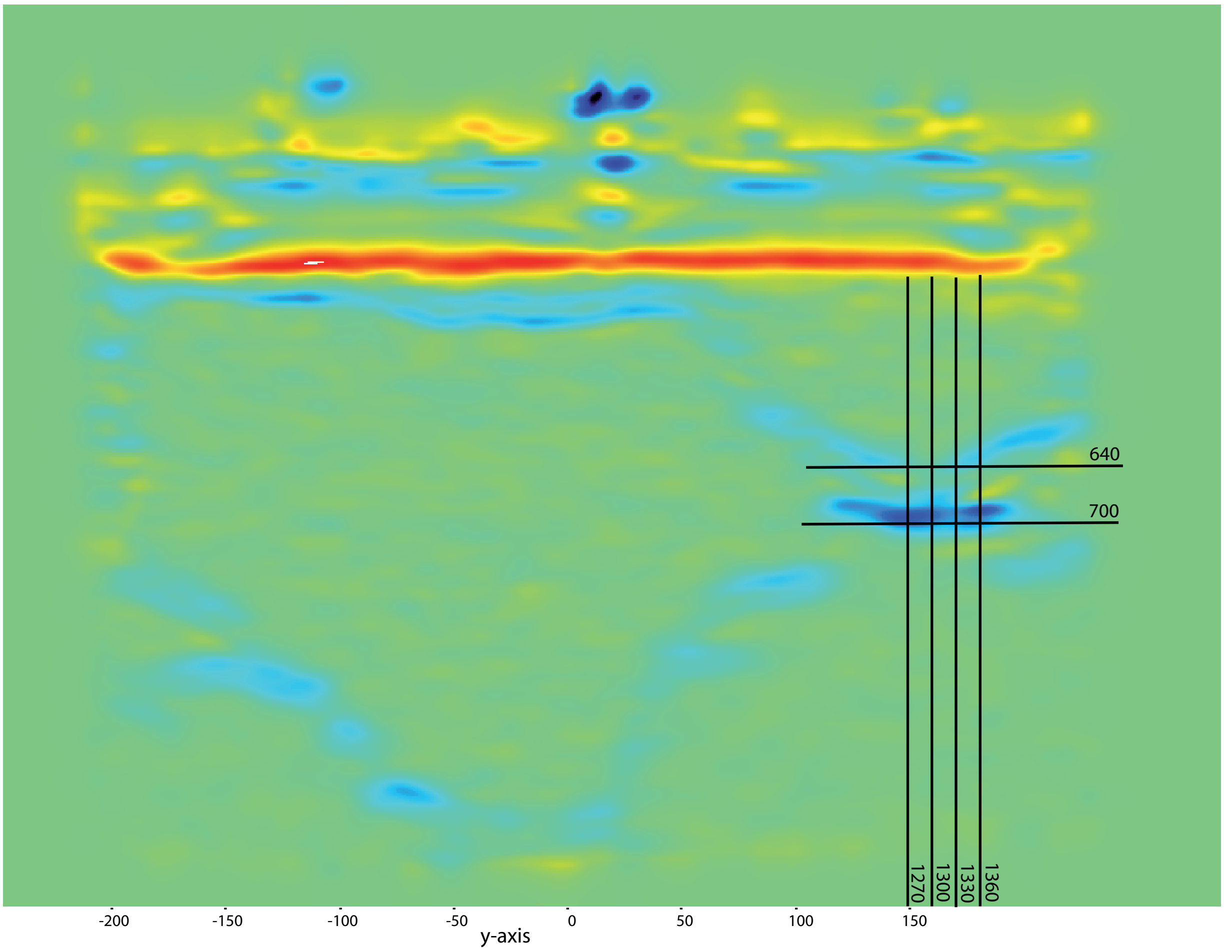

Fig. 8.5 (top): The surface of the experiment is colour coded for strain Exx (at 27.7% bulk shortening). Blue colours indicate locations with high strain accumulation, not coinciding everywhere with the velocity contrasts of Figure 8.2. Black lines show profiles of point locations used in Figures 8.7 and 8.8. Convergence was from top to bottom. Only structures below the piston (red horizontal stripe) are actually part of the experiment.

Fig. 8.6 (bottom): This figure shows strain data extracted across the strain surface (Exx) of Figure 8.5 through the profile position 1300 for each time step. The time increases from top to bottom, and the piston advances from left to right. The oblique white patch marks the steady convergence over time. The black patches indicate locations of high strain accumulation along three structures that are located within the same profile (cf. Fig. 8.5). Within these structures a horizontally striped pattern is defined by several changes from black to grey to black. This shows the successive stages of high and low to no strain accumulation over time.

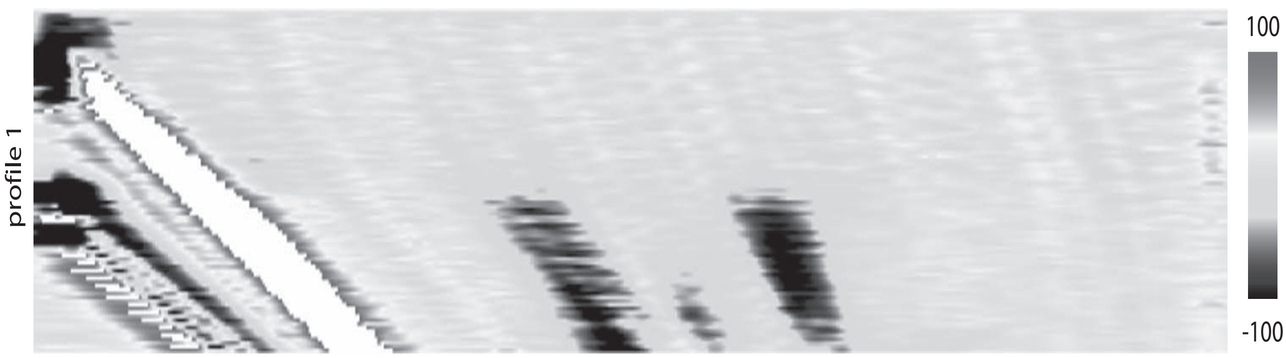

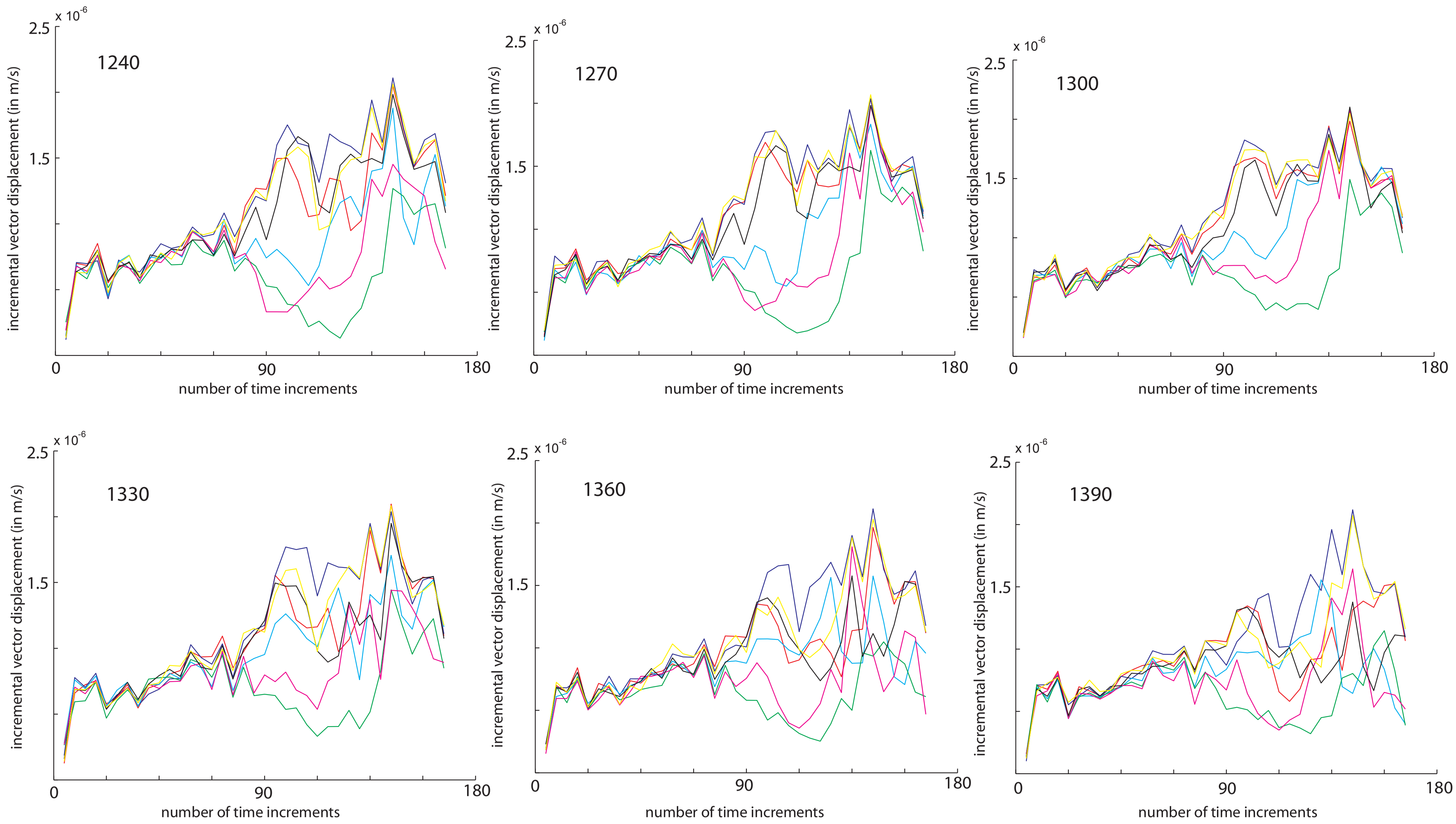

Fig. 8.7: Incremental vector displacement (in m/s) for seven points located in orogen-normal profiles (1240, 1270, 1300, 1330, 1360, 1390, cf. Fig. 8.5 for location of profiles). The x-axis represents the number of time increments equivalent to the observed amount of shortening (180 equals 27.7% of bulk shortening). Colours indicate the position of points along the profile with increasing distance from the piston (blue: 600, yellow: 620, red: 640, black: 660, bright blue: 680, pink: 700, green: 720). Distances between the profile numbers are 30 pixels equalling 9.9 mm; distance between points along profile is 20 pixels (6.6 mm).

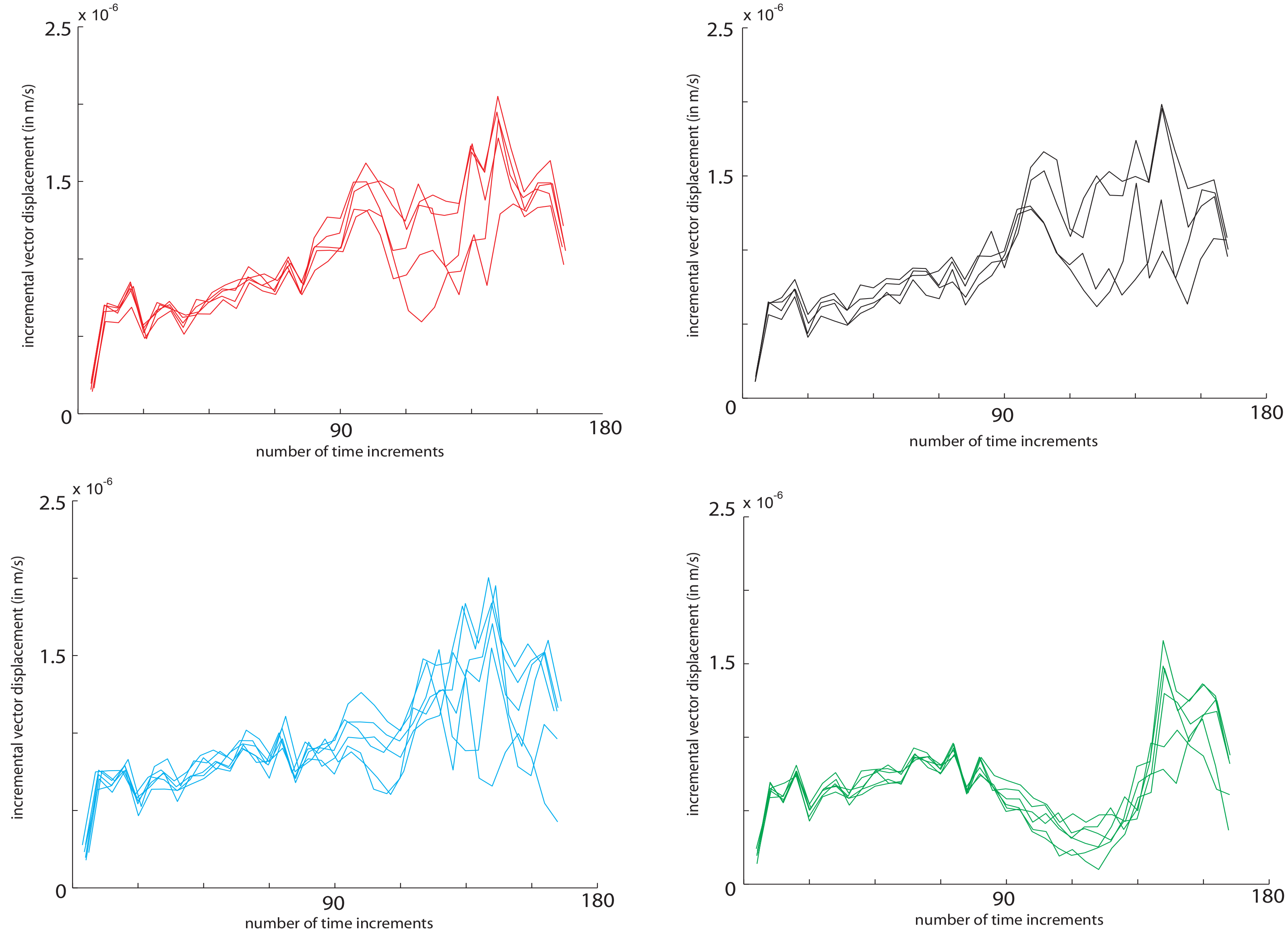

Fig. 8.8: Incremental vector displacement (in m/s) for points located in a profile along-strike (1240, 1270, 1330, 1360, cf. Fig. 8.5 for location of profiles). The x-axis represents the number of time increments equivalent to the observed amount of shortening (180 equals 27.7% of bulk shortening). Colours indicate the position of points along the profile (red: 640, black: 660, bright blue: 680, green: 720). Distances between the profile numbers are 30 pixels equalling 9.9 mm; distance between points along profile is 20 pixels (6.6 mm).